

## **Post-Quench Ductility Study of Zircaloy-4 Cladding under LOCA Conditions**

Yong Yan  
Mike Howell

ORNL Project Manager  
Bruce Bevard

NRC Project Manager  
Michelle Bales

March 2015

This report was prepared as an account of work sponsored by an agency of the United States Government. Neither the United States Government nor any agency thereof, or any of their employees, makes any warranty, expressed or implied, or assumes any legal liability or responsibility for any third party's use or the results of such use, of any information, apparatus, product or process disclosed in this report, or represents that its use by such third party would not infringe privately owned rights.

## Post-Quench Ductility Study of 17×17 Zircaloy-4 Cladding under LOCA Conditions

Y. Yan and M. Howell

March 4, 2015

### 1. INTRODUCTION

The Proposed Rulemaking for revisions to 10 CFR 50.46 includes performance features that require testing of cladding performance under loss-of-coolant accident (LOCA) conditions. The Nuclear Regulatory Commission (NRC) staff has developed regulatory guidance to establish an acceptable test procedure for generating data to develop an analytical limit to meet the proposed rule requirements. The test procedure was largely based on the testing conducted in NRC's LOCA research program [1, 2]. However, some aspects of the draft regulatory guidance were developed with regulatory review in mind and were not addressed by the testing conducted in NRC's LOCA research program—specifically the precision of test conditions needed to support a licensing decision. There is a need to independently execute the test procedures as defined in the regulatory guides so that the staff can evaluate the results and develop informed responses to the public comments on the regulatory guides.

The objective of this research is to execute the guidance documented in DG-1263 and DG-1262 [3, 4] pertaining to the development of an analytical limit for time at elevated temperatures. The testing and evaluation were conducted by following the draft guidelines. The testing includes high-temperature oxidation testing of hydrided cladding material, followed by ring compression testing.

### 2. MATERIALS

The pressurized water reactor Zircaloy-4 cladding tested at Oak Ridge National Laboratory (ORNL) was provided by the Electric Power Research Institute (EPRI). The nominal compositions of commercial Zircaloy-4 cladding are given in ASTM B811, which has 1.20-1.70% Sn, 0.18-0.23% Fe, 0.07-0.13% Cr, and 0.09-0.16% O, with the balance being Zr. The cladding materials that were tested in this program may vary slightly in chemical composition. Table 1 show the characterization of the EPRI Zircaloy-4 specimens before testing, as provided by EPRI and as measured by ORNL.

**Table 1. Characterization of EPRI 17×17 Zircaloy-4 cladding**

Parameter	Outer diameter (mm)	Wall thickness (mm)	Hydrogen content (wppm)	Oxygen content (wppm)	Tin (%)	Chromium (%)	Iron (%)	Hafnium (wppm)
Zircaloy-4	9.50±0.01	0.57±0.01	8-11	≈1310	1.12-1.26	≈0.10	0.20-0.22	≈100

### 3. TEST METHODS AND EXPERIMENTAL APPARATUS

In accordance with NRC DG-1262, sets of two-sided steam oxidation tests at 1200°C were conducted. For 1200°C steam oxidation tests, both as-received and hydrided materials were used. Ring compression tests (RCTs) in accordance with GD-1262 were conducted for post-test oxidation samples.

#### SAMPLE PREPARATION

Test specimens are 25.4 mm long 17×17 Zircaloy-4 cladding samples that were cut from a fresh 914.4 mm long Zircaloy-4 cladding tube or hydrided Zircaloy-4 cladding tubes. Before oxidation, the diameter of each sample was measured with a micrometer to an accuracy of  $\pm 0.02$  mm. The measurements were done at two azimuthal orientations 90° apart at the axial center of each sample. Length measurements were also taken. As stated in Section 4.4 of the DG1262, specimens should be pre-cleaned with chemical detergents or organic solvent followed by water cleaning (see ASTM G2/G3M-6). ORNL cleaned the specimen with pure isopropyl and in an ultrasonic bath with distilled water for 5 minutes. Sample weight measurements were conducted before and after each test with a balance that has an accuracy of  $\pm 0.0001$  gram.

#### STEAM FLOW AND TEST APPARATUS

The steam flow system was designed and fabricated by ORNL to produce two-sided oxidation of samples. Distilled water was used as the steam supply. The draft guide 1262 recommends Grade A water with  $\leq 45$  parts per billion (ppb) oxygen. However it also indicates that Laboratory Type I (distilled and/or deionized) water is also of sufficient for oxidation tests at  $\geq 1000^\circ\text{C}$ . The distilled water used by ORNL was tested to have  $\approx 10$  ppm oxygen content. It is ORNL's recommendation that distilled water should be acceptable and included in the recommendations of the draft guide. . The steam flow rate was derived from water consumption during the test; it was not measured directly. Before sample insertion, the test chamber was flushed with steam to displace air. The schematic of the experimental apparatus is shown in Fig. 1. The furnace is a 48 in. (1210 mm) long resistance furnace with a uniform heating zone  $\approx 150$  mm near the center of the furnace. The test chamber is a quartz tube that contains the sample and the flowing steam. A steam generator is used to produce high-temperature steam at  $\geq 400^\circ\text{C}$ . Steam, at near-atmospheric pressure, flows up through the quartz-tube test chamber at  $5.0 \pm 0.5$  mg/cm<sup>2</sup>/s and exits the chamber into air.

#### MATERIAL HYDRIDING

The hydriding system consists of a tube furnace that can be heated to 400–450°C in the presence of hydrogen to introduce a desired quantity of hydrogen into the sample (see Fig. 2). The heated test chamber facilitates hydrogen absorption by the metal. By controlling the initial hydrogen gas pressure and the temperature profile, the desired hydrogen concentration can be attained. The hydrogen content of the hydrided specimens was measured by using the vacuum hot extraction

(VHE) method according to ASTM E1447-05 and by neutron scattering. The target hydrogen concentrations for hydrided specimens are 150 and 300 wppm.

### NEUTRON SCATTERING TEST

Small-angle incoherent neutron scattering (SAINS) experiments were performed on the beam line of the High Flux Isotope Reactor at ORNL to nondestructively obtain the hydrogen distributions of the hydrided specimens [5]. The neutron wavelength was 6 Å with a wavelength spread of 15% that was set using a Mirrotron (Hungary) velocity selector. Scattered neutrons were collected with a 1×1 m two-dimensional position-sensitive detector with 192×256 pixels, as shown in Fig. 3. The size of the collimated incident neutron beam was defined by a neutron-absorbing pinhole aperture plate placed in front of and next to the sample. The samples were placed in a holder fixed at the proper height and mounted on a motorized sample stage controlled by an instrument computer. The SAINS scattered neutron intensity was obtained by summing the intensities measured in all of the area detector pixels and normalizing the results to the monitor detector counts.

### THERMAL BENCHMARK TEST

Temperature control and monitoring are extremely important in conducting oxidation-quench tests, because the time-at-temperature for the transition between ductile and brittle behavior is a strong function of temperature. Because the sample has such low thermal mass per unit of length, it is important to ramp to the hold temperature at a relatively fast rate for these tests without temperature overshoot due to the initially rapid heat generation rate from cladding oxidation. In setting the controller parameters, the requirements are that the temperature overshoot during the ramp be <20°C relative to the target hold temperature for a short period of time (a few seconds) and that the average hold temperature be within ±5°C of the target temperature. For tests conducted at 1200°C, temperature overshoot was minimized by slowing down the heating rate at ramp temperatures within 50–100°C of the target temperature.

Figure 4 shows the thermal benchmark results for the 1200°C oxidation test, for which one Type-S thermocouple was directly welded onto the sample surface and another Type-S thermocouple was strapped to the sample holding boat. The ramp times to reach the hold temperature were short compared with the hold times at these temperatures, except for the tests with hydrided samples at 1200°C. The average cooling rate to the 800°C quench temperature was  $\approx 12 \pm 2^\circ\text{C/s}$ . The temperature-time curves were used to calculate the Cathcart and Pawel (CP) predicted weight gain and ECR values. After the benchmark test was completed, only the Type-S thermocouple was strapped onto the boat that holds the samples to perform the water quench with the samples in the data generating tests.

### RING COMPRESSION TESTS

Following the high-temperature steam oxidation and water quench,  $\approx 7 \pm 0.2$  mm long rings were cut from near the middle of the 25.4 mm long samples. RCTs were performed at  $135^\circ \pm 1^\circ\text{C}$  at a displacement rate of 0.033 mm/s. A permanent strain (permanent diameter change in the loading direction) can be used as a direct measure of ductility. The sample was unloaded after the first significant load drop indicating through-wall failure along the length of the sample. The post-test diameters along the loading direction were measured directly and compared with the pre-test diameter to give a direct measure of permanent strain. For samples without a tight crack (see DG-1262), offset strain can be used to determine the ductility. The load-displacement curves were analyzed by the traditional offset-displacement method used in analyzing tensile-test data, as detailed in DG-1262. The offset displacement was normalized to the outer diameter (9.50 mm) to give a nominal plastic hoop strain.

## 4. RESULTS

### STEAM OXIDATION TESTS AT $1200^\circ\text{C}$

Table 2 lists the test matrix for oxidation of samples for post-quench ductility tests. For as-received specimens, the times and ECR values listed correspond to those calculated using the CP weight gain correlation, a nominal wall thickness of 0.57 mm, and two-sided isothermal oxidation in steam. Figure 5 shows the temperature histories (monitor TC) of steam oxidation tests NRC#6, NRC #7, and NRC#8 with as-received materials; the histories indicate that the test conditions (heating RAMP and cooling rates) are the same for all of them.

For hydrided specimens, targeted ECRs were calculated based on the hydrogen concentrations within samples and the derived values from Fig. 2 of NRC DG-1263. Neutron scattering was first used for nondestructive evaluation of the hydrogen concentration and distribution on 150 mm long hydrided tubing samples to select uniform hydrided areas for post quench ductility (PQD) study. This approach allowed us to predetermine the target ECR values and corresponding test times. The hydrided samples selected from neutron scattering were then sectioned into  $\approx 25.4$  mm long specimens for oxidation tests. Two 1 mm long rings were cut from the areas immediately adjacent to both ends of each 25.4 mm long hydrided oxidation specimen; hydrogen concentrations for the rings were analyzed by the standard VHE method. The hydrogen concentrations of the hydrided samples listed in Table 2 were obtained by the VHE method, which is in excellent agreement with the hydrogen concentrations determined by neutron scattering [5]. From the measured hydrogen concentration, one can calculate a desired target ECR based on Section 10 of the DG-1262 and Section B of the DG-1263.

Table 3 lists the measured weight gain and ECR values vs. predicted ECR values for the Zircaloy-4 samples oxidized at  $1200^\circ\text{C}$ . Figure 6 shows the weight gain results for Zircaloy-4 vs. the CP predicted values. For the longest test times, the difference between the measured and CP-predicted values is less than 10%. These variations are within the experimental uncertainties and meet the parameters stated in DG-1262.

**Table 2. Test matrix for oxidation of samples for post-quench ductility tests at 1200°C.** The relationship between ECR (%) and normalized weight gain ( $\Delta w$  in  $\text{mg}/\text{cm}^2$ ) is  $\text{ECR} = 1.538 \Delta w$  for 0.57 mm thick cladding samples.

Test ID	Materials	Hydrogen concentration (wppm)	Derived ECR from DG-1263* (%)	Target CP ECR for testing (%)
NRC#6	As-received	$\approx 10$	$\approx 18.5$	18
NRC#7	As-received	$\approx 10$	$\approx 18.5$	19
NRC#8	As-received	$\approx 10$	$\approx 18.5$	20
NRC#10	Hydrided	156 (148–164)	13.3	12.3
NRC#11	Hydrided	160 (152–168)	13.2	14.2
NRC#13	Hydrided	290 (288–292)	9.3	8.3
NRC#14	Hydrided	295 (287–303)	9.2	10.2

\* See Section B of DG-1263

**Table 3. Weight gain ( $\Delta w$  in  $\text{mg}/\text{cm}^2$ ) and measured ECR (%) values for Zircaloy-4 oxidized in steam at 1200°C.**  $\text{ECR} = 1.538 \Delta w$  for Zircaloy-4 (0.57 mm wall)

Test ID	Material	Target CP-ECR (%)	Calculated* CP-ECR (%)	Measured weight gain** ( $\Delta w$ ) ( $\text{mg}/\text{cm}^2$ )	Measured ECR (%)
NRC#6	As-received	18	18.1	10.8	16.7
NRC#7	As-received	19	19.4	11.6	17.9
NRC#8	As-received	20	20.2	11.9	18.4
NRC#10	Hydrided	12.3	12.5	7.7	11.8
NRC#11	Hydrided	14.2	14.2	8.8	13.5
NRC#13	Hydrided	8.3	8.5	5.2	8.0
NRC#14	Hydrided	10.2	10.4	6.5	10.0

\* Calculated ECR is based on the CP-calculation from the temperature history and the benchmark test.

\*\* Measured weight gain is direct measurements of mass changes in samples before and after the oxidation test.

## RING COMPRESSION TESTS

After oxidation tests, 7 mm long rings were cut from the central region of the sample listed in Table 3 for ring compression testing. These tests were conducted at 135°C and a cross-head displacement rate of 0.033 mm/s. The load-displacement curves for these tests are given in Appendix A. These curves were analyzed by the standard offset-displacement method described in NRC DG-1262. Analyses of the load-displacement curves in Appendix A and post-test physical examination of the samples were used to determine the offset and permanent displacement values. These values are listed in Table 4. The permanent strain values were derived from the diameter decrease in samples with a single, tight through-wall crack, which was measured after the test along the loading direction.

As defined by the DG-1262, rings that exhibit  $\geq 1.0\%$  permanent strain are classified as ductile. The value 1.0% is based on uncertainties in diameter readings, on recoil (or spring-back) of cracked rings vs. intact rings, and on diameter reduction due to flaking off of oxide. The ductile-to-brittle transition CP-ECR is defined as the CP-ECR corresponding to 1.0% permanent strain (i.e., the maximum CP-ECR for which ductility is retained). For multiple data points obtained from an oxidation sample, the average permanent strain can be calculated.

For samples that had open cracks or were crushed into pieces, measurement of post-test diameter was impractical and unreliable. In that case, offset displacement and strain were used to assess whether a ring was ductile or brittle. The method for determining the offset displacement has an inherent error because the unknown unloading slope will always be less than the loading slope. It has been demonstrated that the error associated with offset strain displacement increases with calculated oxidation level (see Section 12 of DG-1262). In this work, we used the following ductility criterion (Eq. [3] in DG-1262), based on offset strain:

$$\text{Average measured offset strain} \geq 1.41 + 0.1082 \text{ CP-ECR} \quad (1)$$

Based on the permanent-displacement data presented in Table 4, it is clear that all oxidized samples of as-received materials should be classified as ductile when the ECR is  $< 20\%$  because the measured permanent strains are high ( $> 1\%$ ). Also, the measurements were performed on samples with a single, tight through-wall crack.

For hydrided samples, the post-RCT samples had open cracks or were crushed into pieces. Therefore, the offset strain was used to assess the ductility. Based on the offset strains data in Table 5 and corresponding calculated ductility criteria, sample NRC#10 is defined as ductile, sample NRC#11 as brittle, sample NRC#13 as ductile, and sample NRC#14 as brittle. Figures 7–10 show post-test RCT samples from tests NRC #10, 11, 13, and 14.

**Table 4. Ring compression test results for as-received samples oxidized at 1200°C and quenched** (see Table 3). Tests were performed with an Instron on 7 m long samples at 135°C and at 0.033 mm/s. cross-head displacement. For tests that were stopped after the first significant load drop, diameters were measured directly after the test along the loading direction. The decrease in diameter along the loading direction, normalized to 9.50 mm, is shown in the column “Permanent strain”

Material (Do, mm) CP-ECR	Sample ID	Target CP-ECR (%)	Actual CP-ECR %	Offset displacement $\delta_d$ (mm)	Offset strain $\delta_d/D_o$ (%)	Permanent displacement $d_d$ (mm)	Permanent strain $d_d/D_o$ (%)	Comments
As-received Zircaloy-4 (9.50mm)	NRC#6-2	18	18.1	0.41	4.3	0.19	2.0	Tight crack
	NRC#6-3	18	18.1	0.44	4.1	0.25	2.6	Tight crack
	NRC#6-4	18	18.1	0.46	4.8 Ave=4.4	0.22	2.3 Ave=2.3	Tight crack
As-received Zircaloy-4 (9.50mm)	NRC#7-2	19	19.4	0.50	5.3	0.21	2.2	Tight crack
	NRC#7-3	19	19.4	0.34	3.6	0.15	1.6	Tight crack
	NRC#7-4	19	19.4	0.41	4.3 Ave=4.4	0.17	1.8 Ave=1.9	Tight crack
As-received Zircaloy-4 (9.50mm)	NRC#8-2	20	20.2	0.40	4.2	0.18	1.9	Tight crack
	NRC#8-3	20	20.2	0.34	3.6	0.13	1.4	Tight crack
	NRC#8-4	20	20.2	0.45	4.7 Ave=4.2	0.14	1.5 Ave=1.6	Tight crack



**Table 5. Ring compression test results for hydrided samples oxidized at 1200°C and quenched** (see Table 3). Tests were performed with an Instron on 7 mm long samples at 135°C and at 0.033 mm/s. cross-head displacement. For tests that were stopped after the first significant load drop, diameters were measured directly after the test along the loading direction. The decrease in diameter along the loading direction, normalized to 9.50 mm, is shown in the column “Permanent strain”

Material (Do, mm) CP-ECR	Sample ID	Hydrogen content (ppm)	Target CP-ECR (%)	Offset displacement $\delta_d$ (mm)	Offset strain $\delta_d/D_o$ (%)	Calculated ductility criterion* (%)	Permanent displacement $d_d$ (mm)	Permanent strain $d_d/D_o$ (%)	Comments
Hydrided Zircaloy-4 (9.50mm)	NRC#10-2 NRC#10-3 NRC#10-4	148 156 164	12.3 12.3 12.3	0.42 0.37 0.34	4.4 3.9 3.6 Ave=4.0	2.8	— — —	— — —	2 halves open crack open crack
Hydrided Zircaloy-4 (9.50mm)	NRC#11-2 NRC#11-3 NRC#11-4	152 160 168	14.2 14.2 14.2	0.16 0.13 0.25	1.7 1.4 2.6 Ave=1.6	3.0	0.09 0.08 —	0.9 0.8 — Ave=0.9	Tight crack tight crack 2 halves
Hydrided Zircaloy-4 (9.50mm)	NRC#13-2 NRC#13-3 NRC#13-4	288 290 292	8.3 8.3 8.3	0.49 0.31 0.30	5.1% 3.3% 3.2% Ave=3.9	2.3	— — —	— — —	4 pieces 2 halves open crack
Hydrided Zircaloy-4 (9.50mm)	NRC#14-2 NRC#14-3 NRC#14-4	287 295 303	10.2 10.2 10.2	0.15 0.09 0.14	1.6% 0.9% 1.5% Ave=1.3	2.5	— — —	— — —	2 halves Tight crack Tight crack

\*Ductility criteria were calculated using Eq. (1) and the CP-ECR values.

## 5. DISCUSSION

RCTs were used to assess the ductility of as-received and prehydrided Zircaloy-4 oxidized at 1200°C. Ductility and hydrogen data presented in this work were used to determine embrittlement oxidation levels vs. hydrogen content for prehydrided samples and were compared with the analytical limits defined in Fig. 2 of DG-1263 (see Fig. 11). The post-quench ductility of Zircaloy-4 decreased with increasing oxygen pickup and ECR, as well as the hydrogen concentration within the specimens. The data points generated with our hydrided Zircaloy-4 are also in good agreement with Argonne National Laboratory data [1], as shown in Fig. 12.

For as-received cladding materials, we conducted oxidation and quench testing at ECRs from 18 to 20% to scope out a zirconium-alloy cladding material's oxidation behavior in the as-received condition. Following the guidance of DG-1262, each oxidation and quench sample was segmented into three RCT samples. The average of these three RCT samples was compared with the ductility criterion defined in terms of  $\geq 1.0\%$  permanent strain, by which specimens oxidized up to 20% can be defined as ductile. The embrittlement oxidation limit shown in Fig. 2 of the DG-1262 is 18%. This value was derived by a dataset including an embrittlement threshold of 16% CP-ECR for an older Zircaloy-4 cladding. For modern as-received cladding, embrittlement thresholds cluster at 19–20% CP-ECR, which is in agreement with our data in this work. More oxidation tests with higher oxidation levels are needed to determine the ductile-to-brittle transition for as-received cladding materials.

Hydrided cladding materials were used to characterize the effect of hydrogen on oxidation embrittlement behavior. In this work, 150 and 300 wppm of hydrogen were chosen as the target hydrogen contents to determine the ductile-to-brittle transition for prehydrided material. We conducted oxidation and quench testing near the transition ECR defined in Fig. 2 of DG-1262 and proceeded to an ECR 1% above and an ECR 1% below this limit. Testing was performed to focus on the ECR range between ductile and brittle results at the transition ECR level. The offset strains of the RCT samples were compared with the ductility criterion defined in DG-1262. Our results are in excellent agreement with the analytical limit given by DG-1262. The pre-hydriding samples oxidized to an ECR 1% above this limit can be classified as brittle, but the pre-hydriding samples oxidized to an ECR 1% below this limit can be classified as ductile. Our results are summarized in Tables 3 and 4 and Fig. 11, in which the open circles represent ductile data points and solid dots represent brittle data points.

## 6. SUMMARY

Oxidation tests were completed for as-received and hydrided Zircaloy-4 samples, which were oxidized in steam at 1200°C, slow-cooled to 800°C and water-quenched to room temperature. The weight gain due to oxidation was in agreement with CP model predictions. Ring-compression tests were performed at 135°C and a displacement rate of 0.033 mm/s to determine post-quench ductility. The RCTs were generally conducted through the first significant load drop indicative of a through-wall crack extending along the length of the sample. The permanent strain and offset displacements determined from the load-displacement curves were used as one measure of ductility. The ductility criterion in DG-1262 was used to assess the ductile-to-brittle transition. Our data with hydrided samples are in excellent agreement with the ductile-to-brittle transition oxidation level (CP-ECR) proposed by DG-1262, as a function of pretest hydrogen

content in cladding metal. Future work will consist of performing more RCTs at 135°C on 1200°C–oxidized-and-quenched oxidation samples with as-received and hydrided Zircaloy-4 cladding materials at different ECR levels.

## REFERENCES

1. M. Billone, Y. Yan, T. Burtseva, and R. Daum, *Cladding Embrittlement During Postulated Loss-of-Coolant Accidents*, NUREG/CR-6967, Nuclear Regulatory Commission, July 2008.
2. Y. Yan, T. Burtseva, and M. C. Billone, *LOCA Results for Advanced-Alloy and High-Burnup Zircaloy Cladding*, NUREG/CP-0185, pp. 97–121, Nuclear Regulatory Commission, June 2004.
3. M. Bales, *Establishing Analytical Limits For Zirconium-Based Alloy Cladding*, Draft Regulatory Guide DG-1263, US Nuclear Regulatory Commission, March 2014.
4. M. Bales, *Testing for Postquench Ductility*, Draft Regulatory Guide DG-1262, US Nuclear Regulatory Commission, March 2014.
5. Y. Yan, S. Qian, K. Littrell, C. M. Parish, and L. K. Plummer, “Fast, quantitative, and nondestructive evaluation of hydrided LWR fuel cladding by small angle incoherent neutron scattering of hydrogen,” *Journal of Nuclear Materials* 460, 114–121 (2015).

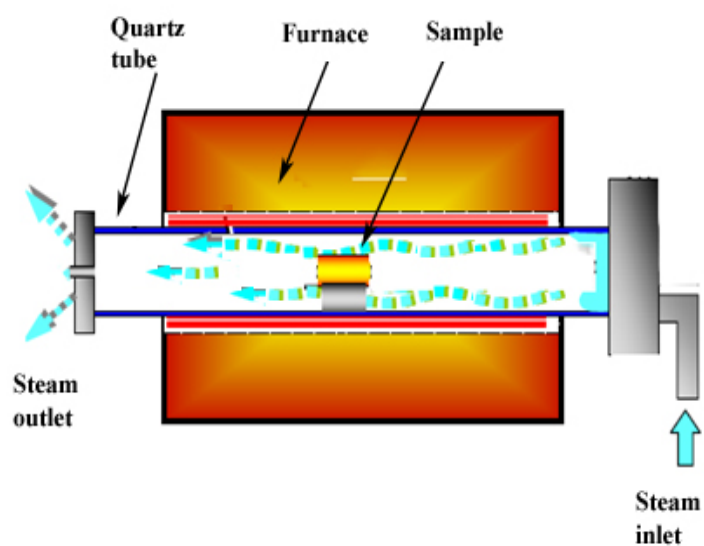


Fig. 1. Schematic of the oxidation kinetics studies apparatus.



Fig. 2. The hydriding system consists of a tube furnace, a stainless test chamber, and a hydrogen generator.

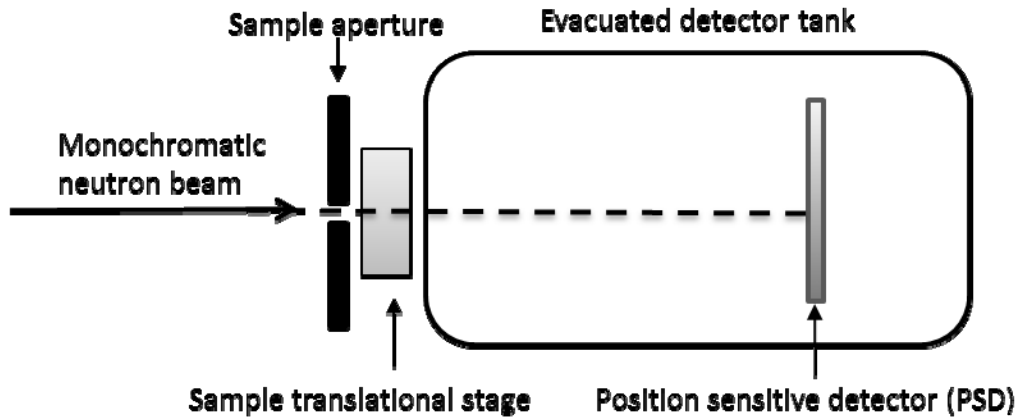


Figure 3. Neutron scattering instrument configuration.

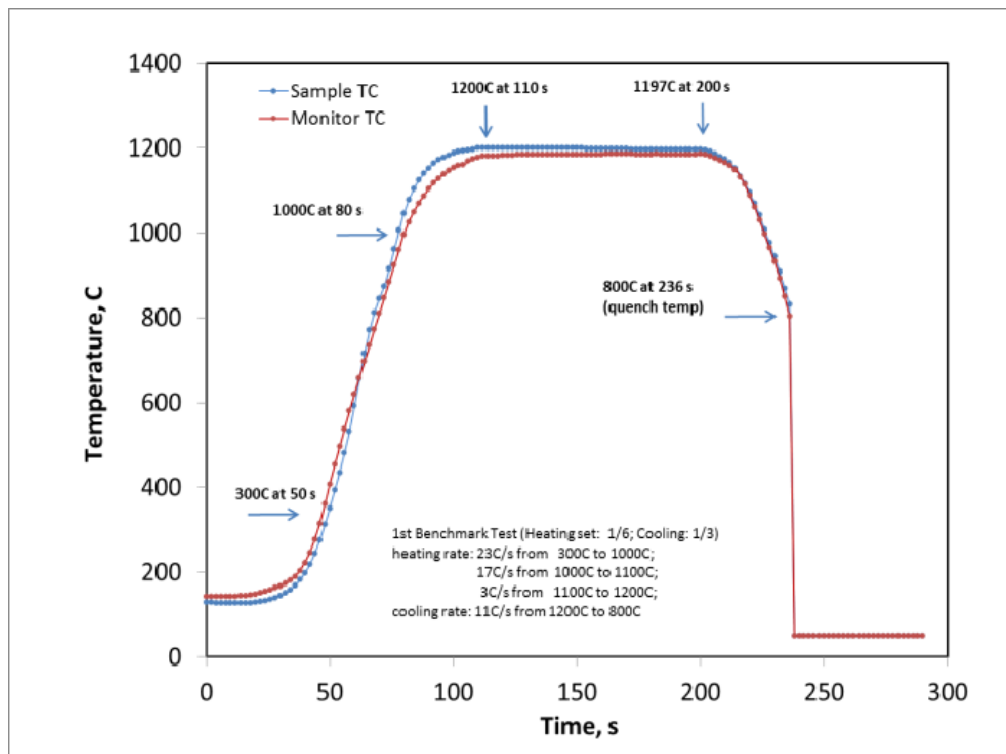


Fig. 4. Thermal benchmark test NRC-B1 with a Type-S thermocouple (Sample TC) welded on sample OD surface (0.51 mm wire). Monitor TC is adjacent to the sample.

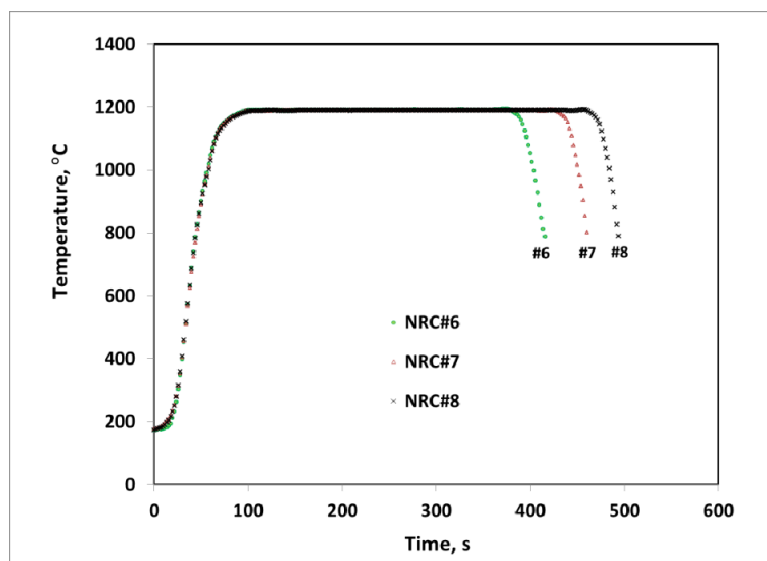


Fig. 5. Temperature histories (Monitor TC) of steam oxidation tests NRC#6, NRC #7, and NRC#8. The samples were water quenched at 800°C.

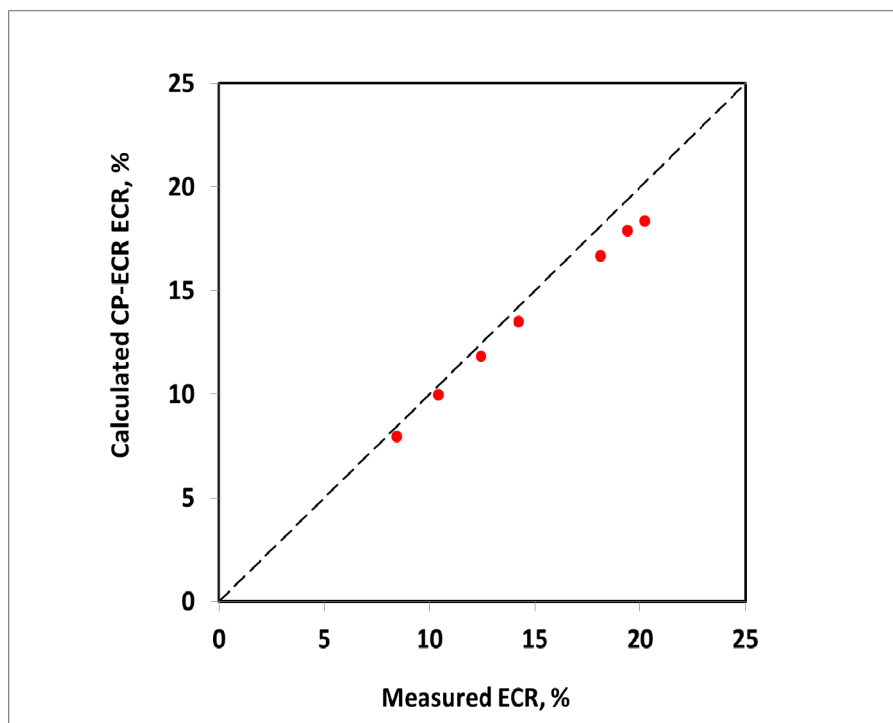
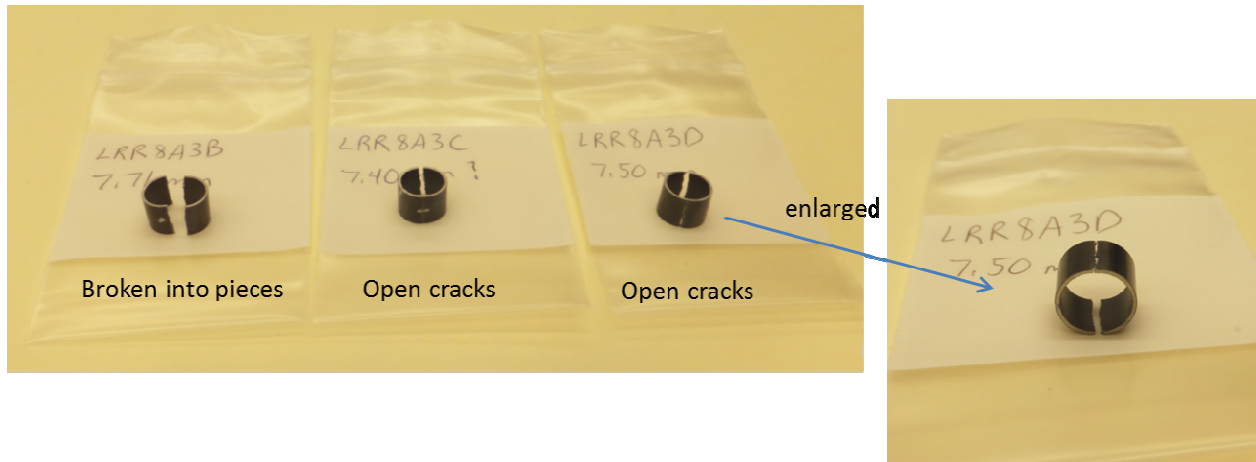
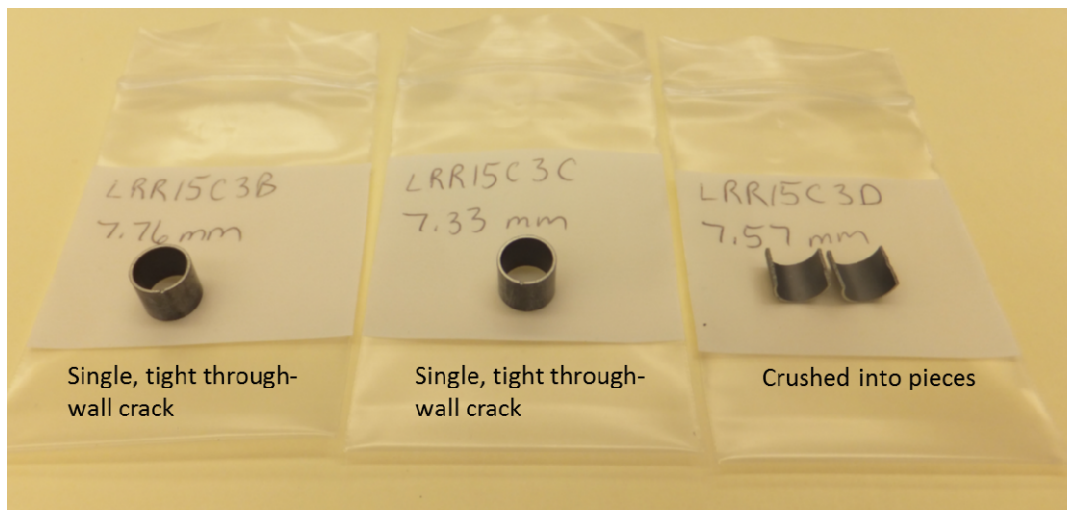


Fig. 6. Comparison of measured and CP-predicted ECR for Zircaloy-4 oxidized at 1200°C.



**Fig. 7. Post-test RCT samples 8A3B, 3C, and 3D from test NRC# 10 (hydrogen concentration: 1448–164 ppm) at target CP-ECR=12.3%.**



**Fig. 8. Post-test RCT samples 15C3B, 3C, and 3D from test NRC#11 (hydrogen concentration: 152–168 ppm) at target CP-ECR=14.2%.**





**Fig. 9. Post-test RCT samples 143E2, E3, and E4 from test NRC#13 (hydrogen concentration: 288–292 ppm) at target CP-ECR=8.3%.**

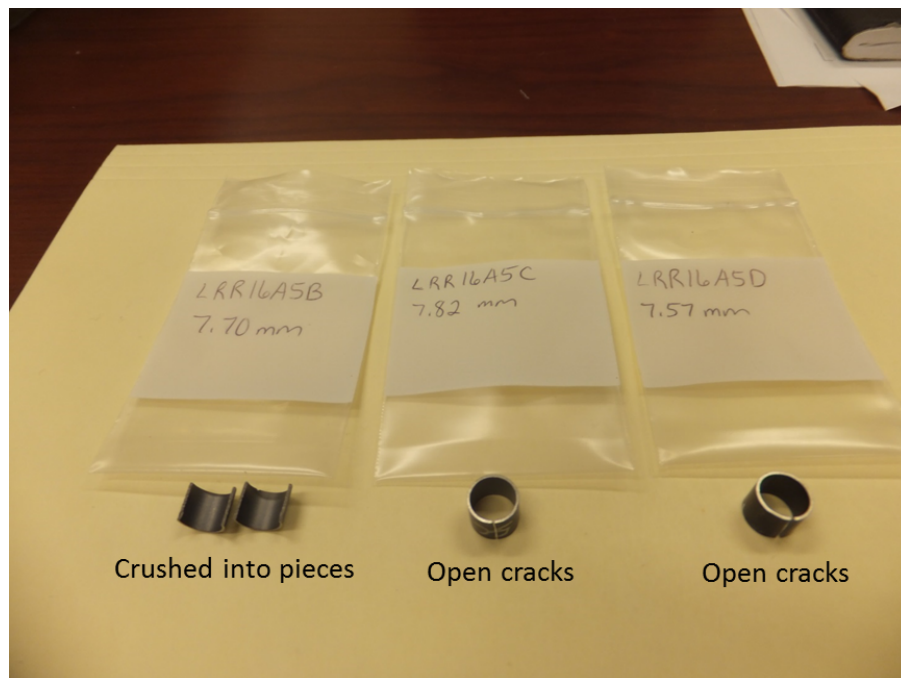


**Fig. 10. Post-test RCT samples 16A5B, 5C and 5D from test NRC#14 (hydrogen concentration: 287–303 ppm) at target CP-ECR=10.2%.**



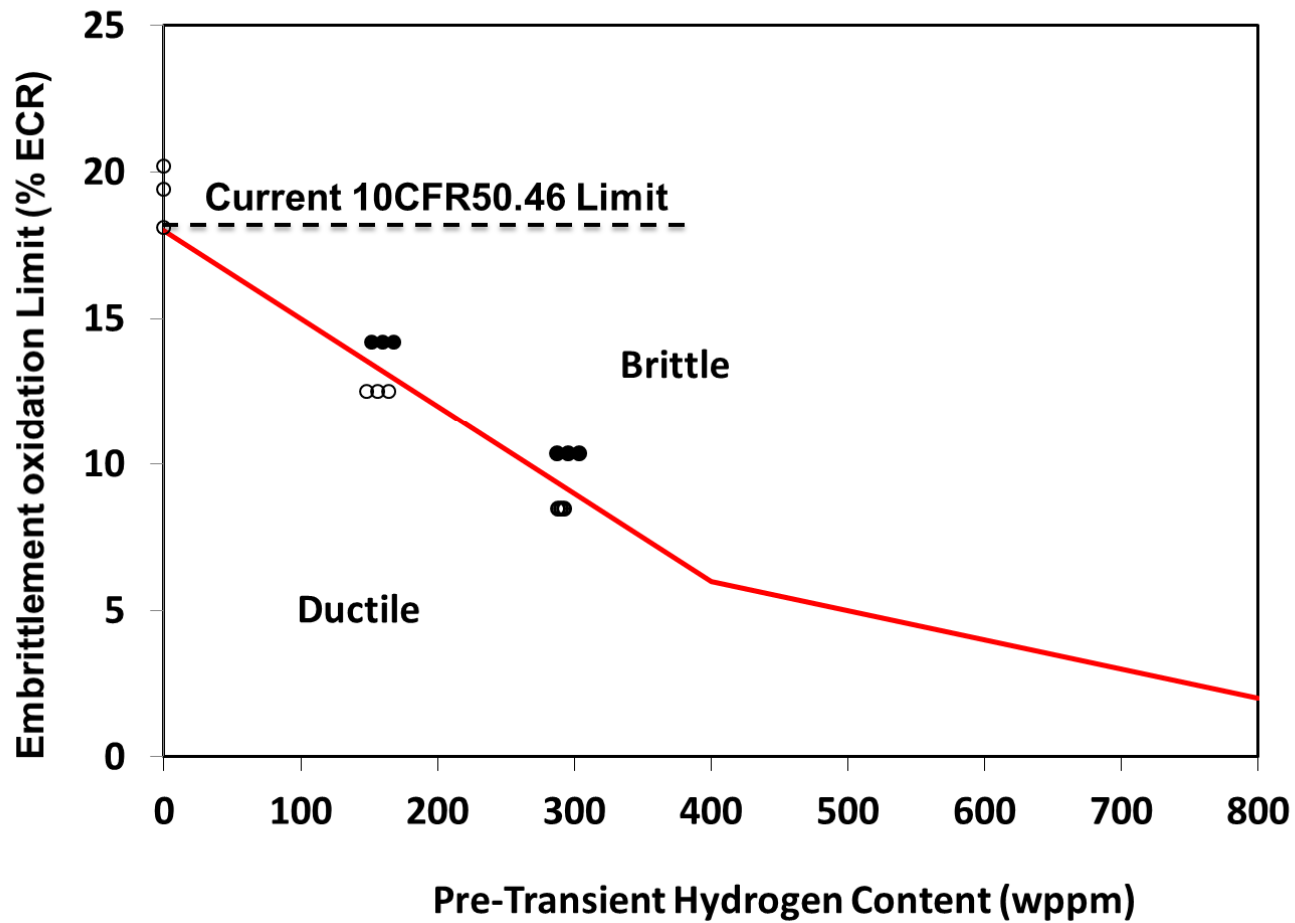


Fig. 11. Ductile-to-brittle transition oxidation level (CP-ECR) as function of pretest hydrogen content in cladding metal for as-received and prehydrogenated cladding materials (see Ref. 3).

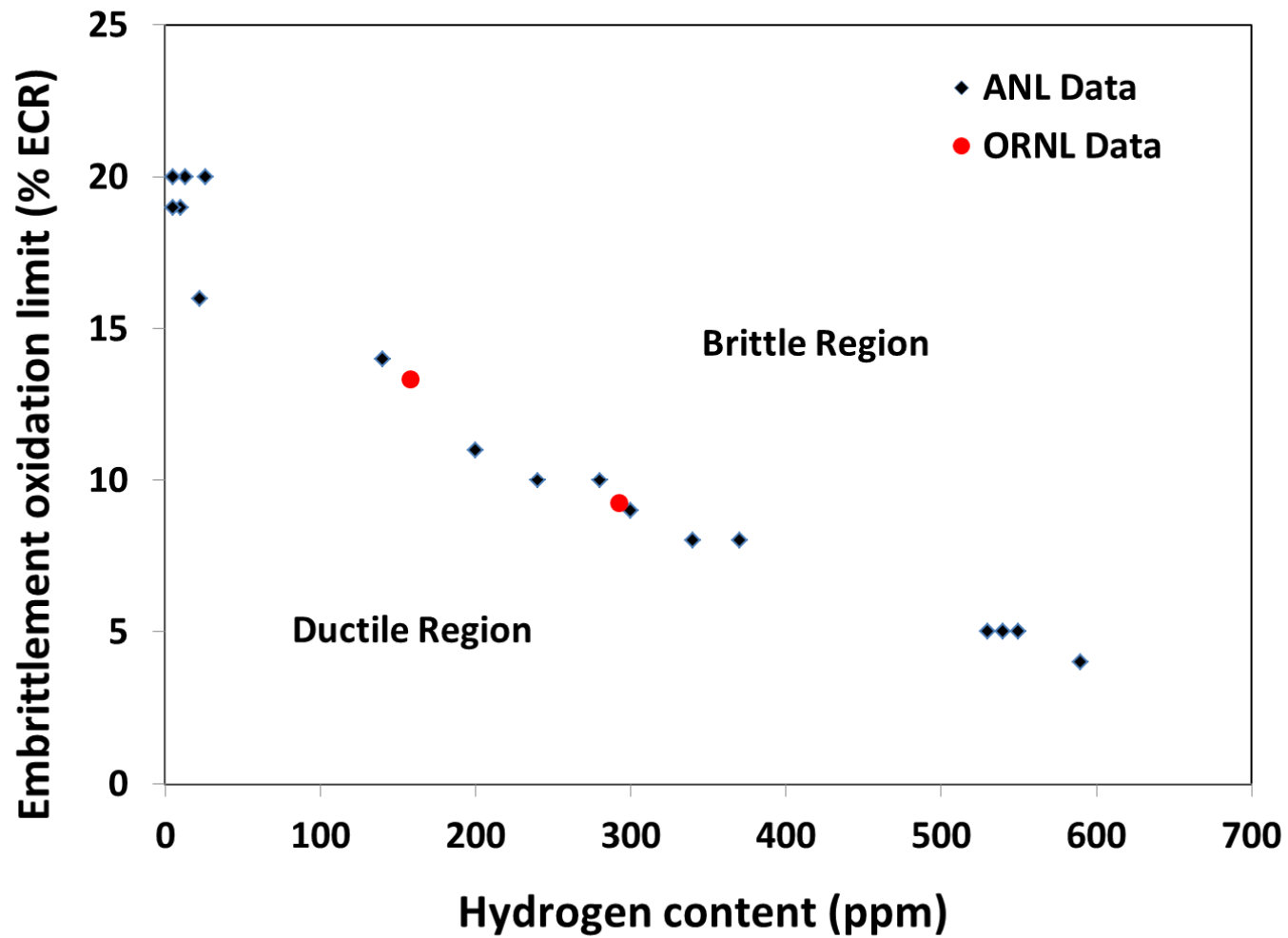


Fig. 12. Ductile-to-brittle transition oxidation level (CP-ECR) as function of pretest hydrogen content in cladding metal for as-received and prehydrided cladding materials.

## **APPENDIX A**

### **Load-Displacement Curves for Oxidized Zircaloy-4 Samples Subjected to Ring-Compression Tests**

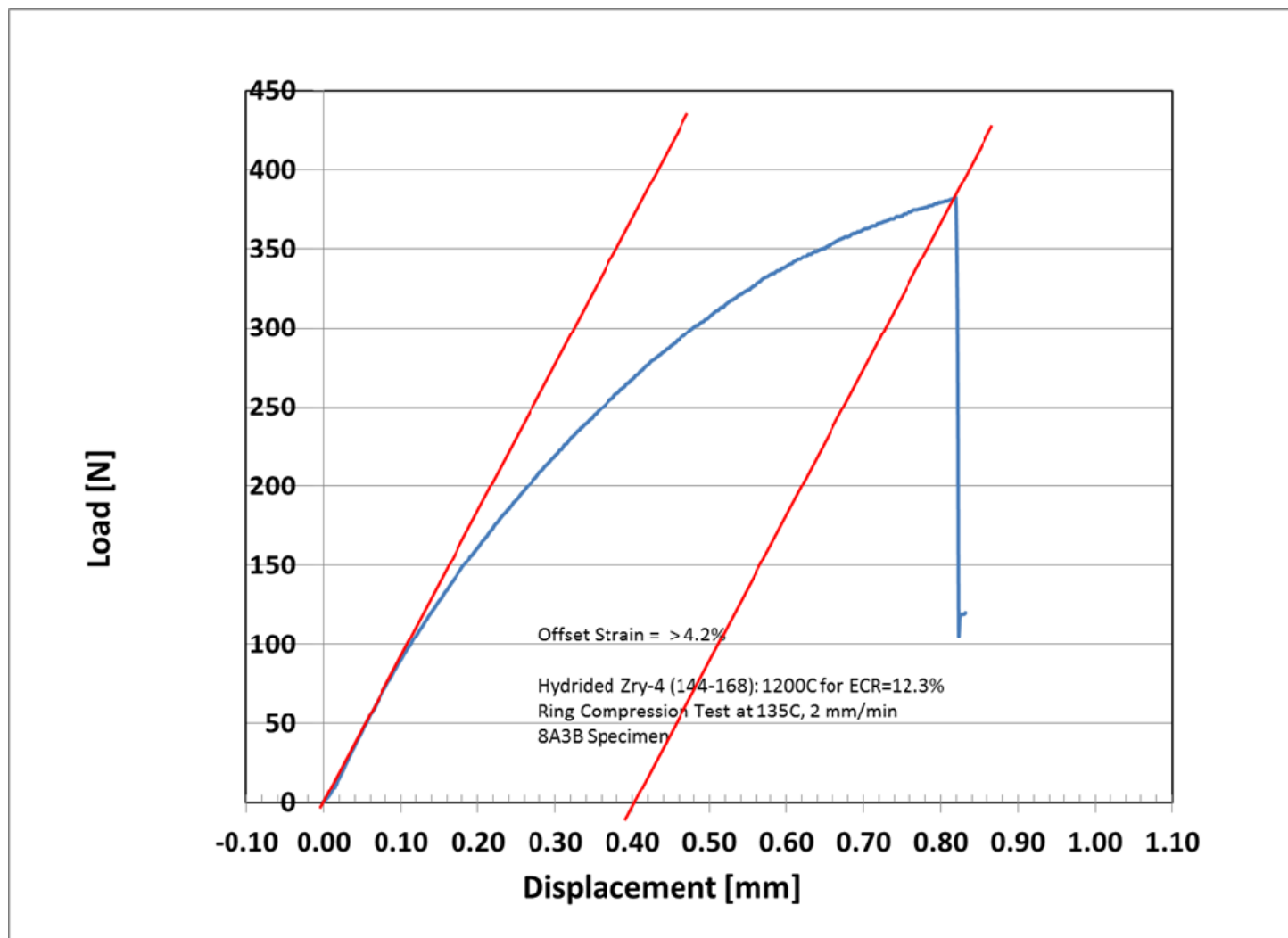


Fig. A.1. Ring-compression load-displacement data for sample 8A3B (test NRC#10) oxidized to 12.3% ECR at 1200°C.

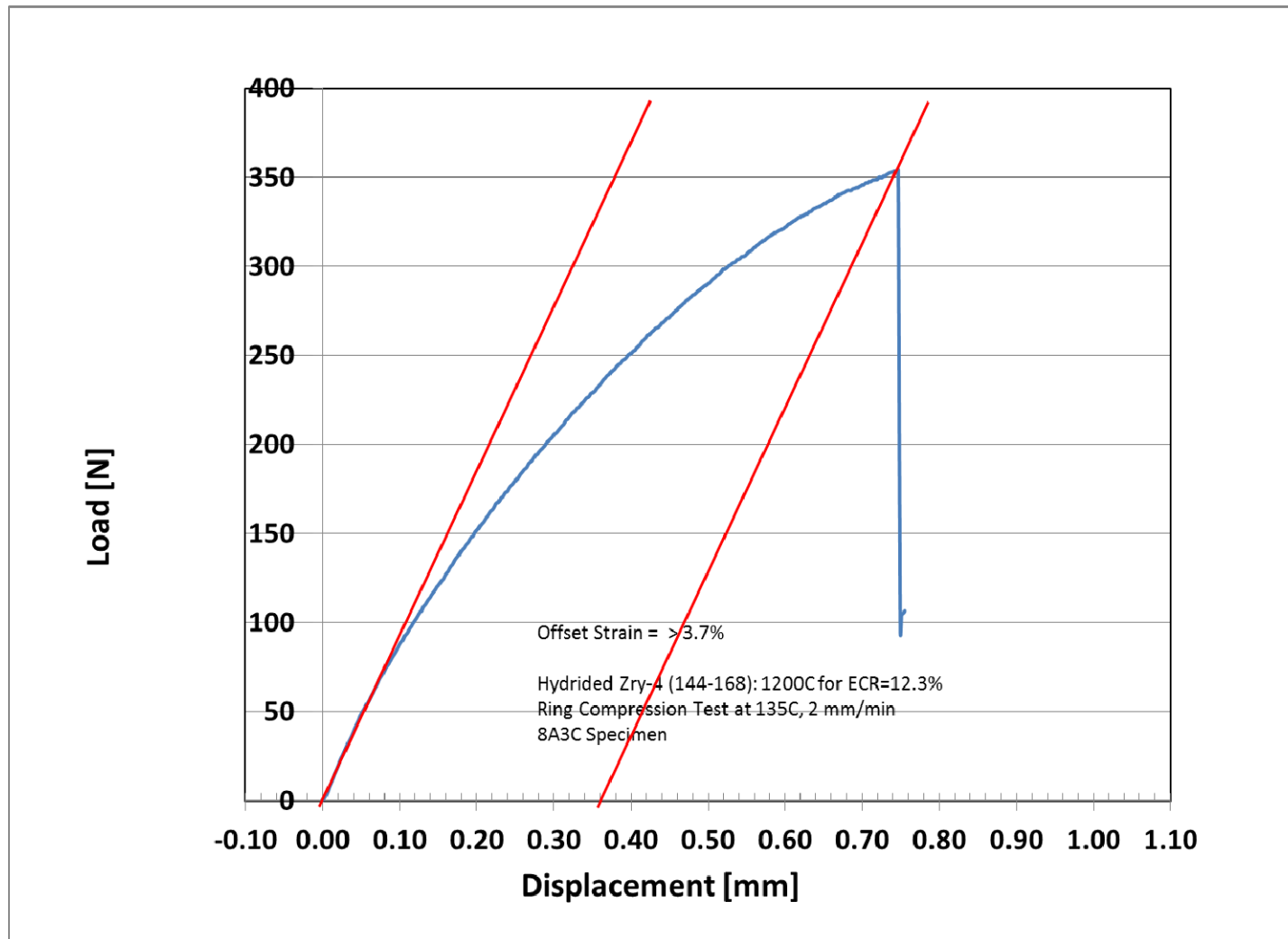


Fig. A.2. Ring-compression load-displacement data for sample 8A3C oxidized (test NRC#10) to 12.3% ECR at 1200°C.

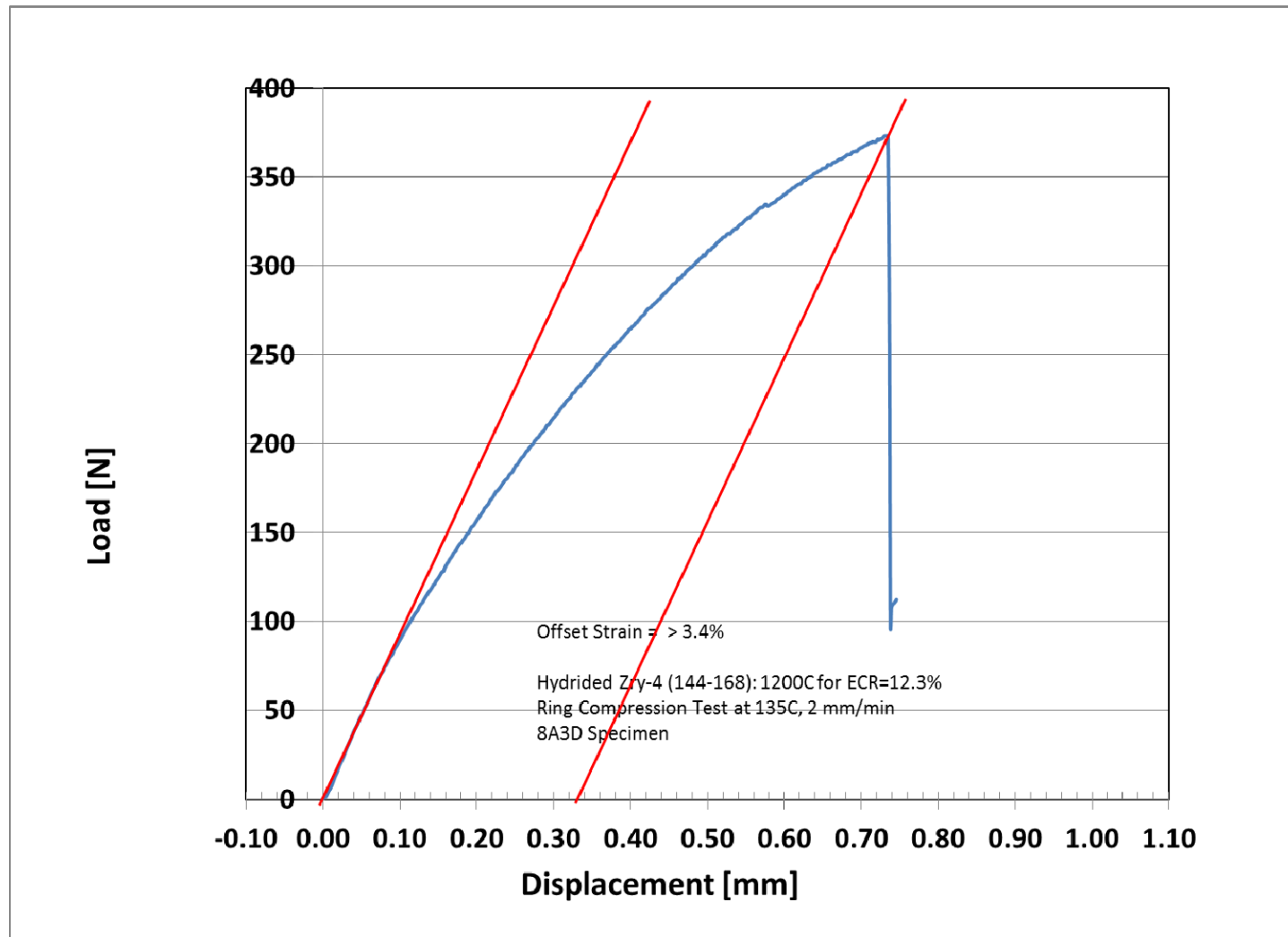


Fig. A.3. Ring-compression load-displacement data for sample 8A3D (test NRC#10) oxidized to 12.3% ECR at 1200°C.

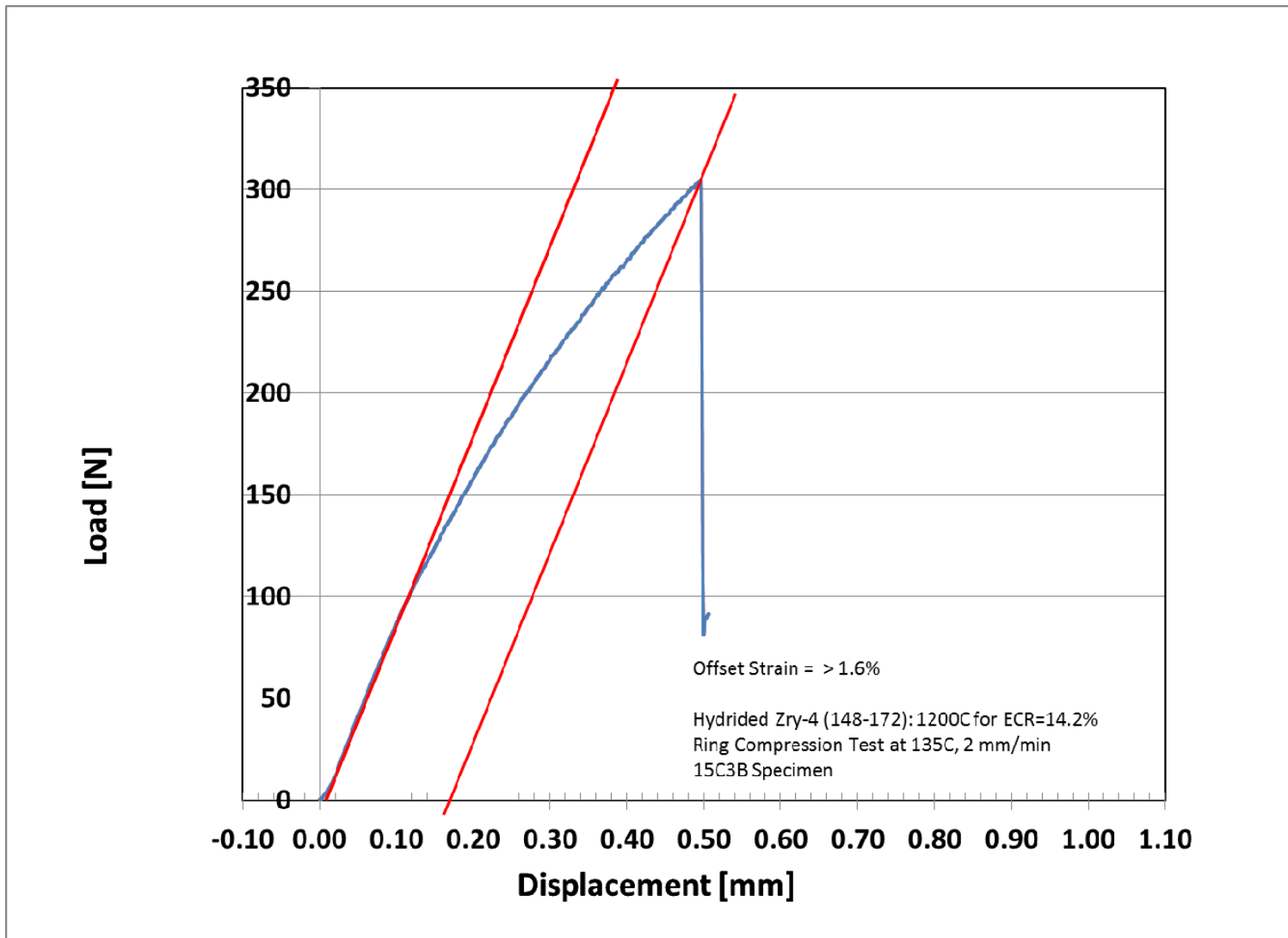


Fig. A.4. Ring-compression load-displacement data for sample 15C3B (test NRC#11) oxidized to 14.2% ECR at 1200°C.

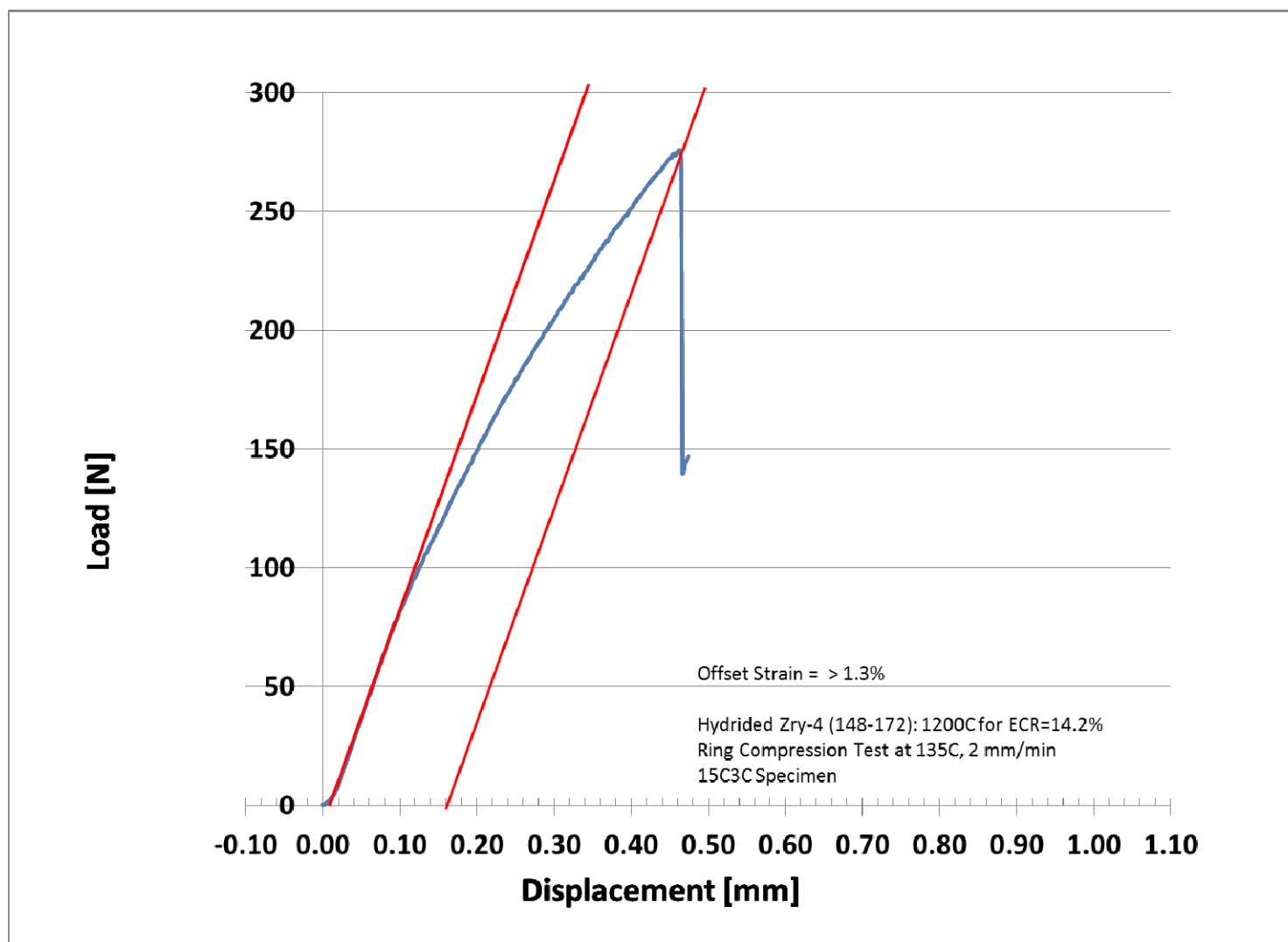


Fig. A.5. Ring-compression load-displacement data for sample 15C3C (test NRC#11) oxidized to 14.2% ECR at 1200°C.



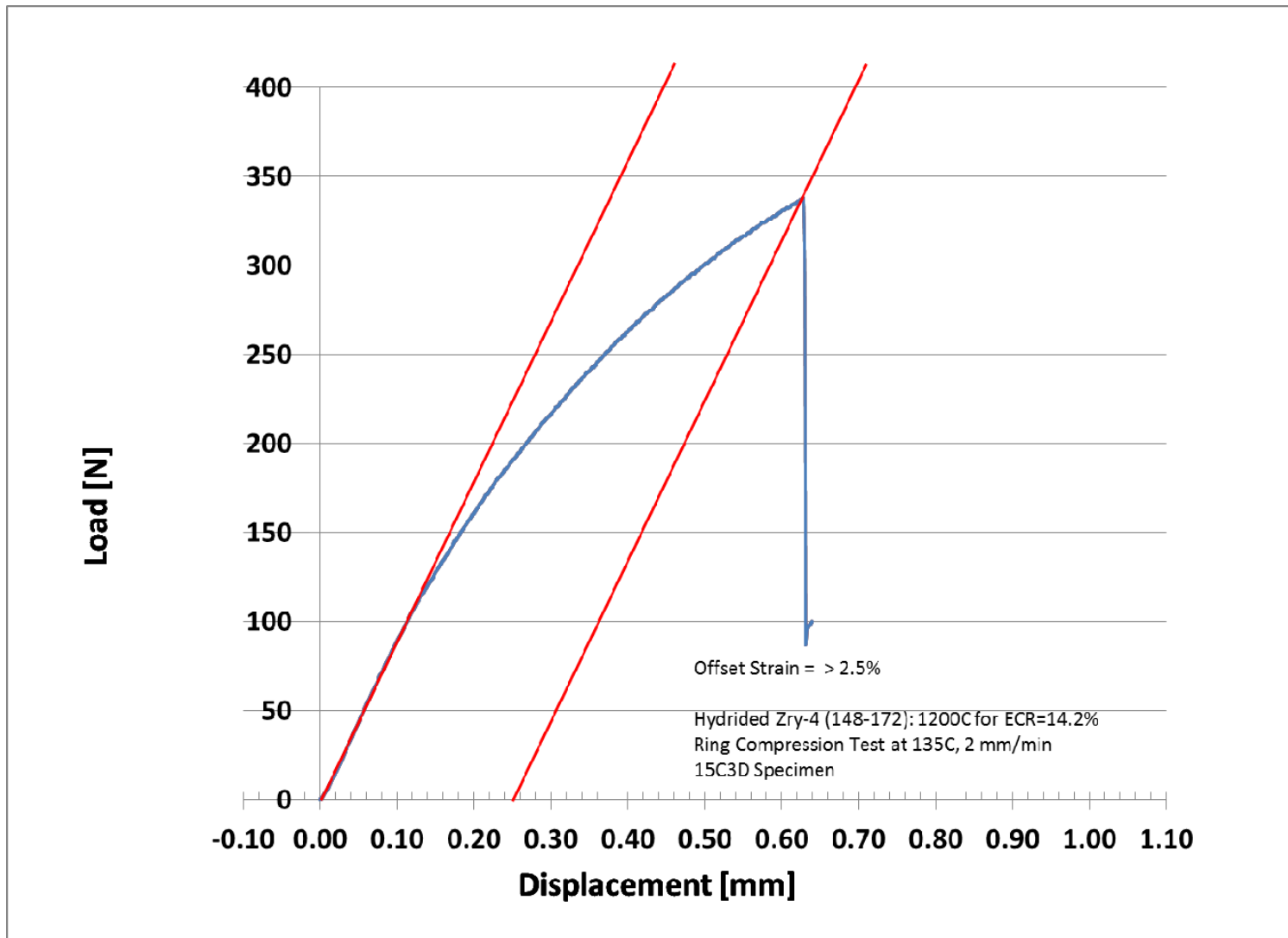


Fig. A.6. Ring-compression load-displacement data for sample 15C3D (test NRC#11) oxidized to 14.2% ECR at 1200°C.